Revue des Composites et des Matériaux Avancés-Journal of Composite and Advanced Materials
Vol. 34, No. 4, August, 2024, pp. 465-480
Journal homepage: http://iieta.org/journals/rcma

Mechanical Characteristics and Durability of Metakaolin-Based Self-Compacting Geopolymer Concrete as A Function of Recycled Aggregate and Steel Fiber Contents

Mohammed Wadi Aljumaili[1*], Salmia Beddu[1], Zarina Itam[1], Jumah Musdif Their[2]

[1] Department of Civil Engineering, College of Engineering, Universiti Tenaga Nasional (UNITEN), Selangor 43000, Malaysia
[2] Anbar Education Directorate, Ministry of Education, Ramadi 31001, Iraq

Corresponding Author Email: PE20940@student.uniten.edu.my

https://doi.org/10.18280/rcma.340408

Received: 12 April 2024
Revised: 1 June 2024
Accepted: 12 June 2024
Available online: 27 August 2024

Keywords:
mechanical characteristics, metakaolin-based, geopolymer concrete, recycled aggregate, steel fiber

ABSTRACT

There has been a significant interest in the development of eco-friendly building materials. Recyclable and environmentally friendly, geopolymer composites are extraordinary binding materials. The purpose of this experimental study was to examine the mechanical and durability properties of metakaolin based self-compacting geopolymer concrete (SCGPC) comprising steel fibers (SF) and recycled aggregate concrete (RCA) varying percentages of recycled coarse aggregate. The mechanical and durability properties of the geopolymer composites, including fracturing tensile strength, and flexural strength, were subsequently evaluated. At weight proportions of 0%, 25%, 50%, 75% and 100%, the recycled coarse aggregates were substituted for the natural coarse aggregates. The amounts of SF incorporated into the mixtures were 0, 0.5, 1.0, and 1.5% by volume fraction. While the incorporation of SF does not yield a substantial improvement in compressive strength, it substantially enhances fracture tensile strength and flexural behavior. The load-displacement graph demonstrated that the incorporation of steel fibers into geopolymer composites increased their fracture toughness, resulting in a higher maximal load capacity. The findings suggest that the incorporation of RCA into SCGPC reduces its flexural behavior, splitting and compressive tensile strengths, and durability, particularly under peak load, deflection, and load. Furthermore, it is observed that RCA negatively synergize with respect to compressive and fracturing tensile strength. However, SF exhibit a significant positive synergy in terms of flexural properties.

1. INTRODUCTION

Concrete, second only to water in terms of usage, necessitates a significant amount of Portland cement. Portland cement production entails significant energy consumption and results in substantial emissions of carbon dioxide (CO_2) and other detrimental greenhouse gases. Therefore, it is crucial to identify an alternative to the current one. Geopolymer is regarded as a substitute for cement that helps mitigate environmental issues [1-3]. It offers the benefits of minimal CO_2 emissions during manufacture and the utilization of significant amounts of industrial waste, in contrast to Portland cement. Hardened geopolymers possess an intricate three-dimensional network structure composed of interconnected tetrahedrons [1]. These substances can exist in an amorphous state, meaning they lack a well-defined crystal structure, or in a quasi-crystalline state, where they have some degree of order. The primary tetrahedrons included silicon oxide (SiO_4), aluminum oxide (AlO_4), and phosphorus oxide (PO_4). Geopolymerization is the chemical reaction that forms geopolymers. It involves an aluminosilicate source (rich in aluminum and silicon) and an activator solution. Typical aluminosilicate sources include: (i) an industrial byproduct of coal combustion, contains aluminosilicate minerals (fly ash) (ii) a glassy byproduct of steel manufacture that may also contain aluminosilicates (slag). Activators are usually alkaline solutions, such as sodium hydroxide (NaOH) or potassium hydroxide (KOH). Acidic activators are also being studied, but alkaline activation is more prevalent. During geopolymerization, the activator dissolves the aluminosilicate source, allowing aluminum and silicon to react and form new, strong covalent connections. These linkages form a three-dimensional network structure like some natural zeolites [4]. Depending on the aluminosilicate supply and activator utilized, several geopolymers can be generated. These changes can affect the material's ultimate qualities. Polysialates are the most prevalent type of geopolymer, created with alkaline activators and characterized by Si-O-Al-O bonding units. Sialate siloxanes and disiloxanes: These have a greater Si/Al ratio (more silicon than aluminum) than polysialates, which is produced by employing certain activator concentrations or changing the aluminosilicate supply. Geopolymers are three-dimensional network structures that are formed through a unique chemical activation procedure. As a result, these

materials have many uses as binders, including construction, industrial heavy metal adsorption, traffic reconstruction projects, radioactive material treatment, and more [5]. Additionally, geopolymers typically have great anti-corrosion properties, high-temperature stability, and immediate excellent strength. Improper compaction and high viscosity of geopolymer concrete may result in its failure, owing to its elevated viscosity [6]. In order to address this concern, the notion of Self-compacting geopolymer concrete was proposed. This unique type of concrete does not require manual compaction. Instead, it naturally flows and compacts due to its own weight [7-9].

Metakaolin is a newly developed pozzolanic cementitious ingredient. It differs from other available cementitious additives since it is manufactured in a controlled environment [10]. Due to its high reactivity and the appropriate proportion of alumina to silica for geopolymerization, metakaolin has gained significant attention as a potential replacement material for geopolymer binder production over the past decade [11]. Metakaolin could potentially serve as a viable precursor material in the geopolymer manufacturing process due to its consistent properties and propensity for reactivity during both its synthesis and progression [12]. The potential of metakaolin geopolymer as an alternative to cement binder was assessed by researchers. It has been disclosed that geopolymer concrete (GPC) exhibited enhanced mechanical conductivity while maintaining a higher porosity than cement concrete. The use of 15% MK in concrete enhances its compressive and flexural strength [13, 14].

Despite their strength, geopolymers are extremely brittle [15, 16]. To overcome this, there are three main approaches: (a) modifying substrates chemically or physically, (b) reinforcing internally, and (c) applying external constraints. Among the three approaches, the last two are typically more effective and economical. Adding fibers to the geopolymer substrate is a method to enhance brittleness by increasing its density and roughness [17]. There are numerous types of fibers readily accessible for commercial use, including either synthetic or natural fibers, glass, nylon, and steel. One crucial factor influencing the absorbing of material energy is the manner in which fibers and cement matrix are bonded. One of the most advantageous attributes of fibers is their capacity to inhibit the spread of fractures. The use of steel fibers is found to result in an increase in the compressive strength of concrete [18].

In the realm of construction industry environmental sustainability, recycled aggregates serve as a viable alternative to natural aggregates when incorporated into concrete formulations [19-21]. As a result, the incorporation of waste materials into concrete mixtures is gaining traction globally. However, the compressive strength of geopolymer composites containing recycled concrete aggregates was found to be poor in comparison to those comprising natural coarse aggregates, according to study [22]. Thus, RCA included geopolymer concretes are needed to be modified [23].

In simple terms, the blending and merging of composites can result in significant and intricate variations in the functional and mechanical characteristics of GPC [24]. As a result, the use of GPC composites in applications pertaining to engineering is restricted. Furthermore, the specific action mechanisms involved in GPC composites at both the mesoscopic and microscopic levels are still poorly understood and require a thorough examination. The present study aims to examine the impact of utilizing MK and steel fibers in conjunction with RCA as a complete replacement for coarse aggregate on the mechanical characteristics and functionality of SCGPC. Mechanical and shrinkage properties of the fabricated samples were systematically investigated. Furthermore, the effect of attacking acids and salts on geopolymer concrete was observed the morphological changes, weight and compressive strength after exposure to salts and acid were investigated. The authors state that there is limited information on the use of steel fibers and RCA together in metakaolin-based SCGPC. This research is considered innovative because of this lack of existing knowledge.

Existing research on steel fiber-reinforced self-compacting geopolymer concrete has mostly utilized natural coarse aggregates [25]. There is a scarcity of data on how RCA interacts with steel fibers in a metakaolin-based geopolymer binder. This information gap impedes the development of sustainable construction materials based on recycled components. This study examines the impact of using MK, steel fibers, and RCA as a complete replacement for natural coarse aggregate **(Impact of combined utilization).** This work expands on earlier research by investigating how RCA interacts with steel fibres in a metakaolin geopolymer matrix. This combined effect has not been fully studied, particularly in terms of mechanical qualities and durability [26, 27]. The study assessed how this combination affects the mechanical qualities of the SCGPC, including as compressive and flexural strength, among others **(Mechanical performance)**. The study tested the SCGPC's durability by subjecting it to severe environments such as acidic or salty situations. Following this exposure, we assessed changes in weight and compressive strength, as well as look for any morphological changes (changes in microscopic structure) **(Durability assessment)**. This study added to the development of sustainable construction materials by investigating the potential of incorporating fully recycled coarse aggregate and steel fibre reinforcement into a geopolymer concrete formulation. This mixture provides a more environmentally friendly alternative to ordinary concrete.

1.1 Materials

The metakaolin was produced through the process of calcination of the kaolin. The collection of kaolin clay was conducted at Al-Anbar, Iraq. The kaolin was initially ground and subsequently heated in a furnace at a temperature of 700°C±20°C for an hour, resulting in the formation of metakaolin Figure 1(a). The mineral composition of metakaolin employed in the study was determined using X-ray diffraction (XRD) spectral analysis. Figure 1(b) shows the largest quantity of SiO_2. Table 1 shows the chemical and physical characteristics of metakaolin. To activate the SCGPC mixtures, an alkaline solution was utilized. This solution was composed of sodium hydroxide (NaOH) and sodium silicate (Na_2SiO_3). The alkaline solution was prepared in advance of its use by 24 hours. A superplasticizer, which was formulated from a polycarboxylic-ether mixture, was employed in all compositions to achieve the required slump value for fresh SCGPC. The superplasticizer had a specific gravity of 1.08±0.02 and a pH value of 7±1. RCA was obtained locally from a demolished structure Figure 1(c). Its particular physical features and size distribution are described in Table 2. The used coarse natural aggregate is seen in Figure 1(e). Fine steel fibers, shown in Figure 1(g), were used in the experimental process to improve SCGPC flexibility.

Table 1. Physical properties and chemical composition of metakaolin

Test Items	Result
SiO_2	52.10
Al_2O_3	43.80
Fe_2O_3	2.60
CaO	0.20
MgO	0.210
SO_3	0.00
K_2O	0.320
Na_2O	0.110
L.O.I	0.990
PH	6.0-8.0
Surface area (m^2/g)	2.540
Specific gravities	2.600

Table 2. Physical properties aggregate

Type	Size (mm)	Specific Gravity S.S.D	Absorption (%)
NCA	5-19	2.65	1.00
RCA	5-19	2.62	2.18

Table 3. Properties of steel fiber

Characteristics	Specification
State	Copper coated
Density	7860.00kg/m^3
Tensile capacity	>2400.00MPa
Shape	Straight
Melt	1500℃
Length	13±1 mm
Dia.	0.2 mm±0.02 mm

The fibers properties are illustrated in Table 3. The mixture used natural sand as the fine aggregate, with a maximum particle size of 4.75 mm. The specific gravity and water absorption were measured at 2.63 and 1.5%, respectively, indicating conformity with the BS.882 criteria. SCGPC production process showing in Figure 1 (h).

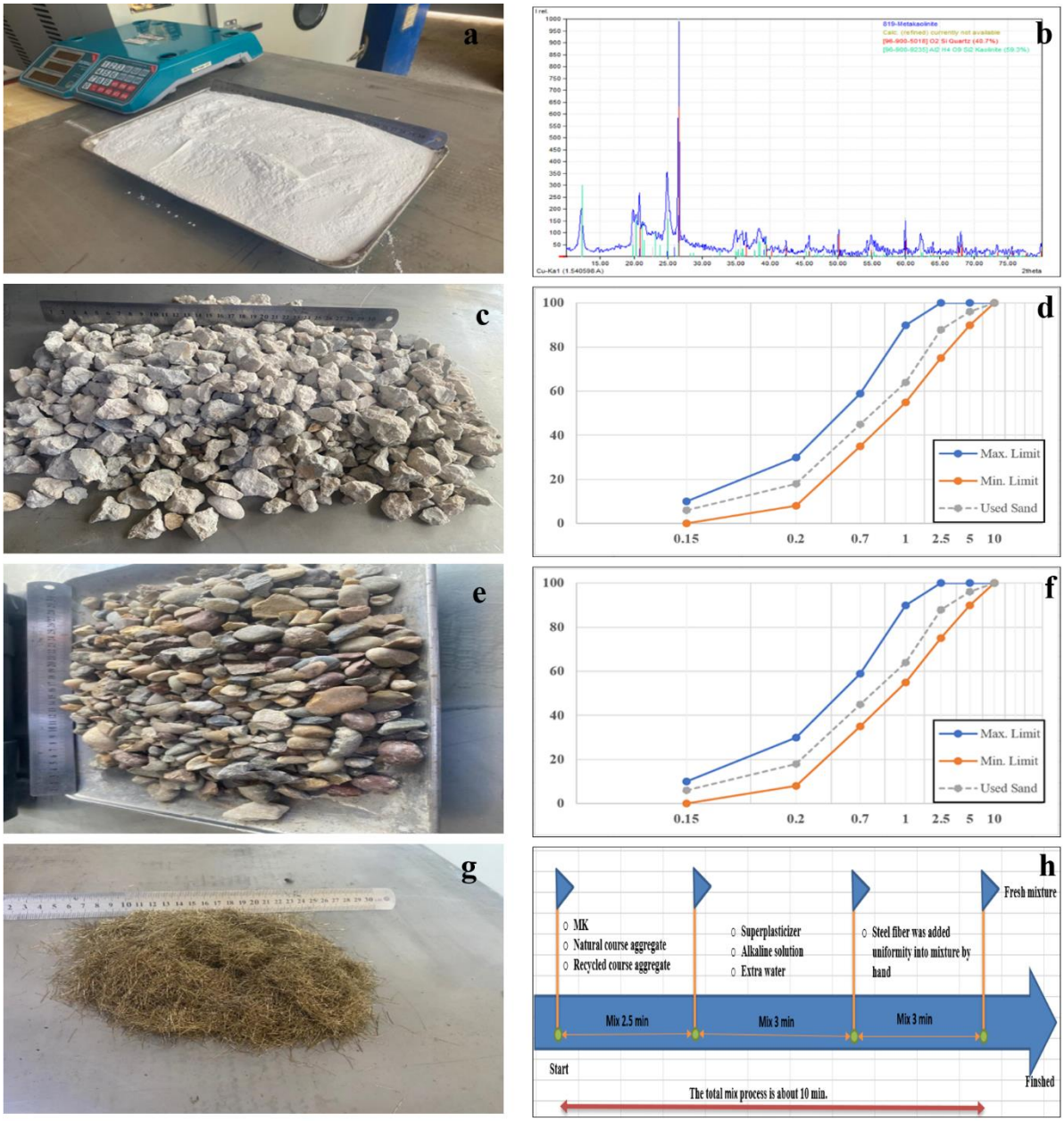

Figure 1. (a) Metakaolin; (b) XRD pattern of metakaolin; (c) Coarse recycled aggregate; (d) Grading of fine aggregate; (e) Coarse natural aggregate; (f) Grading of natural and recycled aggregate; (g) Steel Fiber; (h) Fresh mixture preparation process

1.2 Mix proportions

The research systemically integrated RCA into the sample at different weight percentages (0%, 25%, 75%, and 100%) in place of natural coarse aggregate. Then, varying amounts of SF (0%, 0.5%, 1%, and 1.5%) were mixed with each RCA replacement amount. The total amount of binder used in each batch of SCGPC mixes was 500 kg/m^3, sodium hydroxide concentrations of 12M while curing occurs in lab temperature, 8% superplasticizer, 24% extra-water. The benchmark was a reference concrete mixture made entirely of natural coarse aggregate with no SF added. A comprehensive analysis of all examined concrete mix proportions incorporating RCA and SF is provided in Table 4. Dry ingredients, including aggregates and metakaolin, are combined in a pan mixer for a maximum of 2.5 minutes to initiate the preparation process. Then, a distinct liquid mixture is introduced, which has been pre-mixed and pre-shaken to guarantee uniformity. Typically, this liquid constituent comprises an alkaline solution, a superplasticizer, and extra water. After an additional three minutes of mixing, the mixture is brought into complete uniformity. After verifying the functionality of the recently prepared SCGPC mixture, it is poured directly into molds without undergoing any mechanical compaction. This is due to the self-weight of the mixture being adequate to occupy any empty spaces or compartments. After concrete formation, specimens were covered with a plastic wrap for 24 hours to avoid alkaline solution evaporation. The next day after casting, the samples were taken from their moulds and stored in a curing room with an ambient, controlled temperature until the testing day.

Table 4. Mix proportions of SCGPC

Mix Code	Precursors	Activators		Aggregate			SF
	Metakaolin	NaOH	Na_2SiO_3	NCA	RCA	FA	
RCA0-SF0	500	64.34	160.56	787.3	0	926.6	0
RCA25-SF0	500	64.34	160.56	590.47	196.82	926.6	0
RCA50-SF0	500	64.34	160.56	393.65	393.65	926.6	0
RCA75-SF0	500	64.34	160.56	196.82	590.47	926.6	0
RCA100-SF0	500	64.34	160.56	0	787.3	926.6	0
RCA0-SF1	500	64.34	160.56	787.3	0	926.6	78.5
RCA25-SF1	500	64.34	160.56	590.47	196.82	926.6	78.5
RCA50-SF1	500	64.34	160.56	393.65	393.65	926.6	78.5
RCA75-SF1	500	64.34	160.56	196.82	590.47	926.6	78.5
RCA100-SF1	500	64.34	160.56	0	787.3	926.6	78.5
RCA0-SF1.5	500	64.34	160.56	787.3	0	926.6	117.75
RCA25-SF1.5	500	64.34	160.56	590.47	196.82	926.6	117.75
RCA50-SF1.5	500	64.34	160.56	393.65	393.65	926.6	117.75
RCA75-SF1.5	500	64.34	160.56	196.82	590.47	926.6	117.75

2. SPECIMENS' PREPARATION

Unfortunately, there is no standard test method for directly measuring concrete durability in chemical conditions. However, the ASTM C 267 approach provides a workaround. It is recommended that concrete specimens be pre-saturated in water for 24 hours before being exposed to chemicals. Following this method, the specimens in this investigation were immersed in water for 24 hours and their initial saturated weights were measured. The pre-soaked specimens were separated into three groups and immersed in different solutions (5% sulfuric acid, 5% magnesium sulphate, 3.5% seawater) that simulated harsh chemical conditions. Each group, together with control specimens stored at room temperature, had a 56-day exposure period. To evaluate the concretes' resistance to chemical attack visual inspection, mass change, compressive strength variations approaches were employed.

Fresh properties of SCGPC

The study evaluated the filling and passing abilities of SCGPC mixture concrete by testing its slump flow, V-Funnel, T50 flow, and L-box as showing Figure 2 with varying proportions of MK, RCA and SF, following the EFNARC European guidelines for SC [28].

Hardened characteristics of SCGPC

Research examines the compression, split tensile, and flexural stiffness of SCGPC mixtures by altering the proportions of MK, RCA and SF, shown in Figure 3.

Figure 2. (a) Dlump flow; (b) V-Funnel; (c) T50 flow; (d) L-box

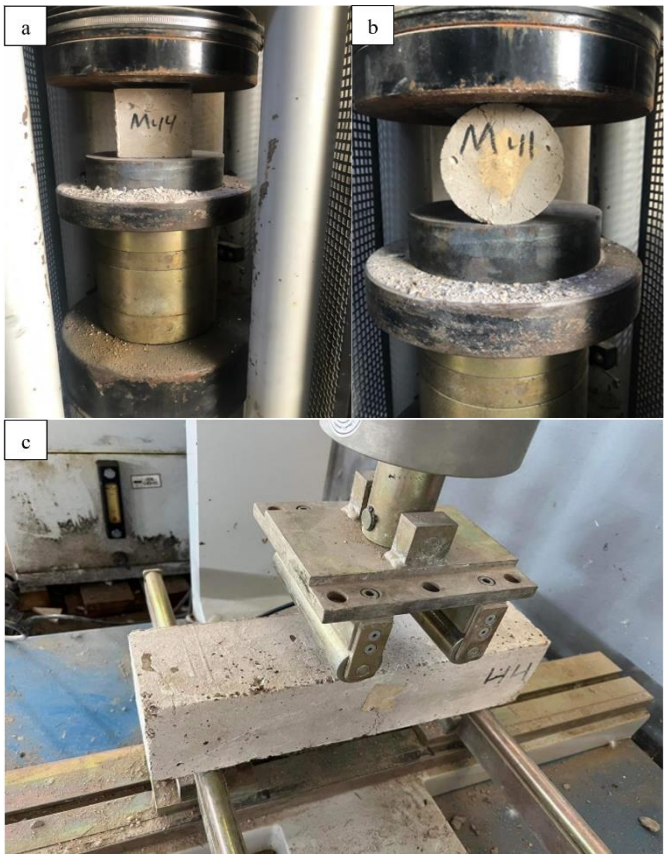

Figure 3. (a) Compressive strength; (b) Tensile strength; (c) Flexural strength

Compressive Strength

In accordance with Kanagaraj et al. [29], we subjected 100 mm cubic specimens to a constant load of 0.25 MPa/s (with a margin of error of 0.05 MPa/s) using a 200-ton digital compression testing equipment.

Tensile strength

Instead of physically pushing on the concrete, an indirect approach known as the splitting tensile test was employed [30] to determine its tensile strength. This entailed applying a steady load of 0.7 to 1.4 MPa/min to cylindrical specimens measuring 100 mm in diameter and 200 mm in height until they shattered.

Flexural Strength:

Following standard [31] we used a four-point loading setup to assess the flexural strength of the SCGPC samples. A steady load of 0.86 to 1.21MPa/min was applied until the specimen failed.

SCGPC's durability characteristic

Concrete's durability and strength are becoming increasingly important for civil infrastructure, especially in severe environments, as previous works have demonstrated. As a result, the concrete utilized in this study was rigorously tested for strength and durability.

Resilience to adverse conditions in the SCGPC

In order to evaluate the harsh environment resistance of he prepared SCGPC, the investigators complied with the methodologies specified in standards [32, 33]. Specimens measuring cylindrical samples (100 mm×200 mm) were subjected to a curing period of 28 days prior to their immersion for 56 days in solutions comprising 5% sulfuric acid, 5% magnesium sulphate, 3.5% seawater. Resistance was evaluated with respect to the following three factors: Visual examination of the shape for physical alterations or damage. Quantifying material loss caused by acid attack involved comparing the mass of each sample to its initial weight. In contrast to samples that were not exposed, the residual compressive strength was ascertained through mechanical testing.

Sorptivity test

The upward flow of water molecules through concrete specimens over time is known as sorptivity. The sorptivity test was conducted subsequently [34]. 100 mm cubic concrete was used for sorptivity measurement. A wax coating was put to the side surfaces of the disks to prevent water absorption and tape was utilized to guarantee full sealing of the treated side. The procedure entailed immersing the disks in a water bath. The water level was adjusted to be positioned one centimeter higher than the bottom of the disks. The initial weight of each disk was recorded at the start of the experiment. Over the course of the next 24 hours, the disks were regularly removed from the water at particular time intervals, such as every 10 or 20 minutes. The rate of water absorption of the SCGPC samples was determined using Equation:

$$I = \left(\frac{m_t}{a/d}\right)$$

It indicates the process of absorption, m_t means the alteration in mass measured in grams, a designates the area of the specimen, and d stands for the density of water.

3. RESULT AND DISCUSSION

3.1 Fresh properties of SCGPC

Slump flow of SCGPC

The ability of SCGPC to smoothly and completely fill complex shapes without requiring vibration is crucial. This mostly relies on the quantity of water in the activating agent solution and the quantity of Superplasticizer used [29]. The slump flow of SCGPC mixtures is represented in Figure 4(a). Among the five mixes, RCA0SF0 sample has the highest recorded value for slump flow (741 mm). This suggests that the mixture has good workability and can easily flow and fill complex forms. The elevated slump value indicates that the mixture was affected by a superplasticizer, which improves its capacity to flow. RCA0SF1.5 has a slump value of 661 mm, which is somewhat lower suggesting that introducing SF may result in a reduction in workability and flowability when compared to the initial mixture. The fine SF particles cover voids between bigger ones, decreasing internal friction and enhancing packing density. However, they also absorb some water required for lubrication. Regarding 0% RCA vs. 100% RCA, the reduction in slump flow from 741 mm to 665 mm indicates some adverse effect caused by the addition of 100% RCA. Possible causes include: RCA has a higher water absorption rate than natural aggregates, which decreases the amount of water available for lubrication and impedes flow. RCA's rougher surface texture and angular shape may enhance internal friction and impede flow compared to smooth, spherical natural aggregates. Overall, all tested SCGPC mixtures showed satisfactory flow and ease of handling.

T_{500} test for SCGPC

The time required for SCGPC blends to pass through a designated channel or section is denoted as the T_{500} test. Frequently, this test is employed to assess the flow

characteristics of SCGPC mixtures. As seen in Figure 4(b) the RCA0SF0 mixture exhibited the shortest concrete flow time of 3.81s. This suggests that the mixture possesses exceptional flowability, as it can pass effortlessly through confined spaces and complex shapes without causing blockages or segregation. However, the incorporation of RCA and SF increases the T_{500} time. The highest T_{50} value was observed at 4.96 s in SCGPC with the highest RCA and SF content (RCA100SF1.5).

V-funnel examination for SCGPC

The V-funnel experiment is a common technique used to evaluate the flow characteristics of SCGPC. The process involves monitoring the duration of time for a newly prepared sample of SCGPC to pass through a V-shaped funnel, as shown in Figure 4(c). This test assesses the concrete's capacity to fill complex shapes without separating or clogging, essential qualities for self-compacting uses.

Examining the V-Funnel Flow findings uncovers intriguing insights into the impact of RCA and steel fiber on flowability. Adding SF and RCA increases flow time in all samples, but when RCA100SF1.5 are present, the flow time is maximum at 12.1s compared to RCA0SF0 11.65s. This may be attributed to various factors, including elevated water absorption and packing density by RCA.

Filling ratio (L-Box)

The L-Box test data were evaluated to figure out the passing ratio of SCGPC samples. Figure 4(d) indicates that all mixes met the EFNARC criteria for filling ability, with a passing ratio ranging from 0.87 to 1.0. 0RCA0SF has a higher filling ratio than samples comprising RCA and SF, showing that the addition of RCA and fiber reduced filling ability.

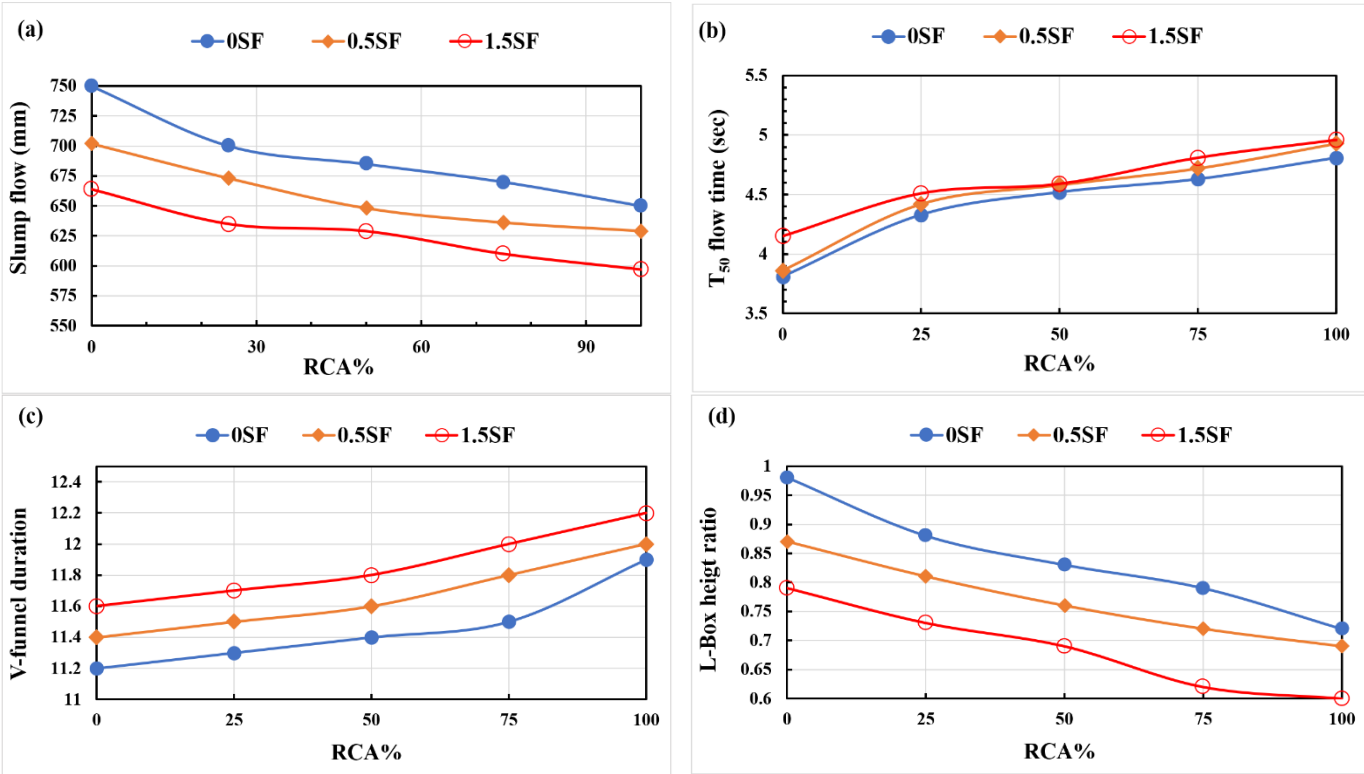

Figure 4. The effect of RCA and SF on (a) slump flow; (b) T_{50} duration; (c) V-funnel duration; (d) L-box height ratio

3.2 Hardened properties of SCGPC

Compressive Strength

Figures 5 (a) and (b) show the impact of SF and RCA quantities on the compressive strength of SCGPC at different curing times. It is discovered that the compressive strength of SCGPC at 7 days about 70% of that at 28 days, suggesting that early curing days are where strength development mostly happens because to a quick hydration reaction. SCGPC mixes with RCAs showed reduced strength compared to mixes without RCAs. SCGPCs made with 100% RCA had a compressive strength that was 50%-55% lower after 7 days and 50%-60% lower after 28 days when compared to mixtures made without RCA, respectively. The reduced strength of concrete mixtures with RCA in comparison to those without RCA is consistent with preceding research on plain concrete. This is attributed to the presence of weak interfacial transition zones (ITZs) in the microstructure of concrete with RCA, which occur among the aggregate and the past mortar that was included to the RCA, as well as between the fresh mortar and the aged mortar [35]. In general, when RCA contents rise, SCGPC's compressive strength tends to drop, while SF contents rise [18]. SCGPC mixes labeled RCA0SF1.5, RCA50SF1.5, and RCA100SF1.5 with 1.5% steel fiber showed a 26%, 28%, and 41% increase in 7-day compressive strength and a 27%, 37%, and 45% increase in 28-day compressive strength compared to equivalent mixes without steel fiber. There is an improvement in compressive strength of SCGPC's that occurs when SF is added, often falling within the range of 30-40%. This rise is most likely because to the It can be concluded that the fibers could bridge across the cracks and arrest the crack face separation during the crack propagation [36]. The improvement in compressive strength is minimal when the SF content increases from 0% to 0.5%, but becomes significant when the SF ratio grows from 0.5% to 1.5% as shown in the Figure 3. This finding is aligned with other reported researches [26, 37, 38]. These findings show that even at a 100% substitution rate, the strength decrease of the concrete caused by replacing natural course aggregate NCA with RCA may be compensated for by appropriately

constructing mixes with steel fiber.

Splitting tensile strength

The fluctuation in splitting tensile strength of SCGPC's follows a pattern similar to compressive strength, with a notable increase due to SF content (Figure 5). The 7-day splitting tensile strengths of RCA0, RCA50, and RCA100 mixtures with 1.5% steel fiber were 36%, 38%, and 48% higher, respectively, compared to the peer unreinforced mixtures. For 28 days splitting tensile strengths of RCA0, RCA50, and RCA100 mixtures with 1.5% steel fiber were 35%, 37%, and 39% respectively. The SF percentage has a considerable effect on the splitting tensile strength of SCGPC due to the SF crack-bridging effect, particularly with elevated SF contents. Introducing SF greatly enhances the splitting tensile strength of SCGPC, with the impact becoming more pronounced as the SF percentage increases. Furthermore, the inclusion of RCA reduces the splitting tensile strength of SCGPC's. At a RCA value of 50%, the rate of change decreases gradually, ranging from11.52% to15.5% for 7 days curing and 4.5% to 9% for 28 days curing. It should be noted that the reducing rate is lower for SCGPC consisting higher content of SF. Studies have demonstrated that replacing natural aggregate with RCA in concrete mixes consistently results in lower splitting tensile strength, regardless of whether the concrete is conventional, self-compacting, or reinforced [37, 39, 40]. This is because using RCAs weakens the interface transition zone (ITZ) between the aggregate and geopolymer pasta, lowering the concrete's total tensile strength. To put it simply, the strength of a composite material is determined by the amount of each component used: density, recycled aggregate, sand, steel fiber, and water. Any modifications to these amounts will cause the compressive strength to fluctuate. The compressive strength is an indirect measure of the composite's other qualities. Figure 5(e) depicts the relationship between the compressive and tensile strengths of concrete formed from recycled aggregate and metakaolin. The chart shows a significant association, with a regression coefficient near to one (83.76%). This validates the statistical analysis.

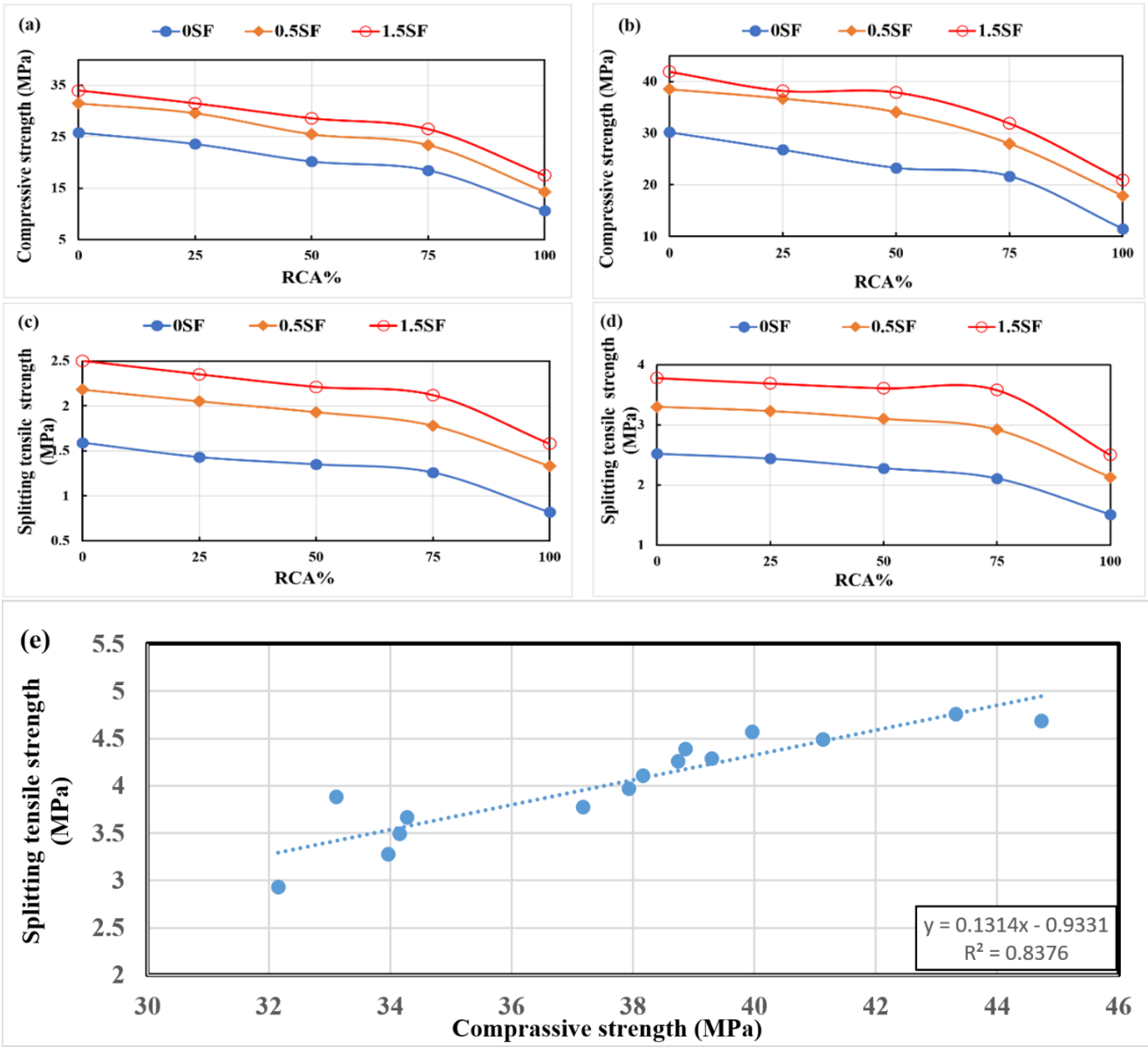

Figure 5. (a, b) Compressive strengths; (c, d) Splitting strength of different mixes at 7 and 28 days; (e) Statistical analysis of the relationship between compressive and tensile strength using regression analysis

3.3 Flexural behavior

Load-deflection curves

Figure 6 displays the load-deflection characteristics of SCGPC samples with varying proportions of RCA and SF. Each curve depicts the mean response of test specimens assessed after 28 days of the curing process. The findings demonstrate that the SCGPC samples saw a substantial load reduction after peak load. Mixes that contained more RCA content experienced a greater load decline after peak load in comparison to those with less RCA ratio. Mixes with 1.5% steel fiber experienced a less noticeable load drop than those with 0.5% steel fiber. Mixtures with a higher RCA may have higher load drops due to RCAs' poor strength, whereas mixes with a higher SF may have lower load drops due to steel fibers' fracture bridging ability [41]. After peak load, the tooth-shaped curve shows that the steel fibers are slowly being drawn out of the paste matrix [42]. An increase in SF ratio resulted in a rise in the residual flexural load of concrete, as shown in the Figure 6(b), for a given RCA ratio. Additionally, it is demonstrated that for a SF, the residual load of the concrete was reduced by adding RCA and reduced further by increasing RCA. Table 5 comprehensively analyses the primary flexural mechanical characteristics obtained from these graphs, including peak load, maximum deflection, residual strength, and related toughness. To explore the behavior of SCGPC subsequent to its attainment of maximum flexural strength, this research presents three distinct residual flexural loads. The loads are designated as PL/300, PL/150, and PL/100, which are equivalent to 1, 2, and 3 millimeter deflections, respectively. This methodology is in accordance with the guidelines specified in the ASTM C1609/C1609M-2012 code [43]. The flexural toughness of a substance denotes its resistance to flexural deformation and fracture. The quantity is determined by taking the integral of the load-deflection graphs until a specific deflection value is reached [44]. Figure 6(a) shows that the load-deflection graphs of SCGPC can be separated into two stages: the rising branch and the falling branch. SCGPC specimens without SF show only the beginning, rising part of the load-deflection curve in Figure 6(b). The load quickly declines to zero at the apex, indicating fragile behavior. In contrast, SCGPC specimens with SF exhibit a definite falling apart after the apex, indicating more ductile behavior. Figures 6(b) and (c) shows that SF and RCA content substantially impact the flexural behavior of SCGPC. As the RCA content increases, the slopes of the first ascending parts of the load-deflection curves and peak loads decrease for all SCGPC samples. Interestingly, for SCGPC with 0.5% SF, the initial ascending branches overlap for all RCA contents. However, the descending branches show significant variances. This shows that increasing RCA concentration diminishes SCGPC ductility, whereas increasing SF content reverses this effect, considerably improving peak and residual loads.

Table 5. Main flexural mechanical properities of SCGPC

Specimen	Peak Point			Residual Load			Toughness		
	δ_{peak} (mm)	P_{peak} (kN)	f_{peak} (MPa)	P_{L300} (kN)	P_{L150} (kN)	P_{L100} (kN)	Ω_{L100} (Joule)	Ω_{L150} (Joule)	Ω_{L300} (Joule)
RCA0-SF0	0.638	20.64	5.272				6.086		
RCA25-SF0	0.633	19.73	5.020				5.581		
RCA50-SF0	0.622	18.84	4.811				5.363		
RCA75-SF0	0.607	18.33	4.681				4.987		
RCA100-SF0	0.581	17.21	4.392				4.402		
RCA50-SF0.5	0.738	20.50	5.231	10.624	2.817	0.411	18.067	16.613	11.116
RCA50-SF1.5	0.702	20.84	5.322	13.133	6.940	3.846	25.975	21.957	11.337
RCA0-SF1.5	0.773	22.50	5.741	17.307	8.905	4.925	30.946	24.536	12.419
RCA25-SF1.5	0.742	21.32	5.443	14.34	8.413	4.432	29.382	23.532	12.383
RCA75-SF1.5	0.674	18.64	4.760	9.986	4.140	1.936	19.097	16.22	9.781
RCA100-SF1.5	0.644	19.60	5.001	6.696	1.979		13.382	12.903	8.808

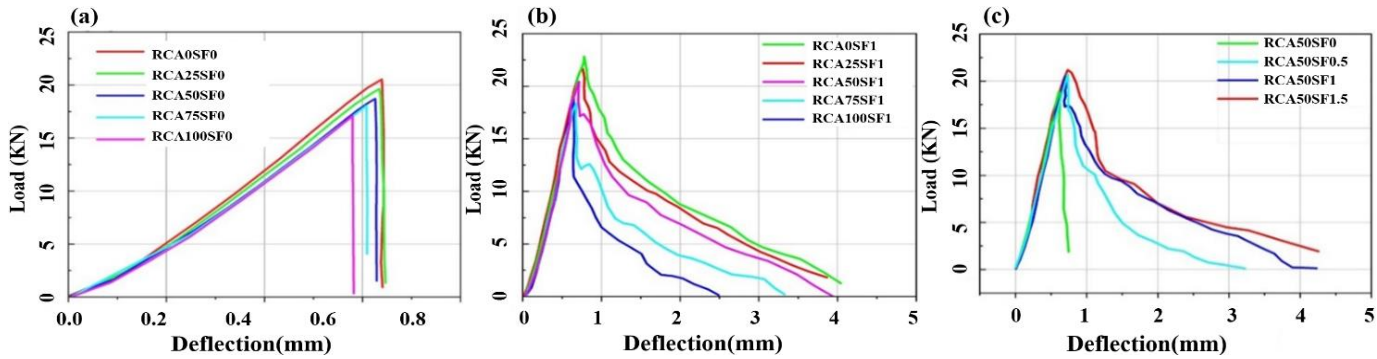

Figure 6. Load-deflection graphs of (a, b) Impact of RCA ratio; (c) Impact of SF ratio

Load and deflection properties

Figures 7 and 8 display the maximum flexural strength and peak deflection of SCGPC with different amounts of SF and RCA. Clearly, the flexural strength and peak deflection of SCGPC are reduced when the RCA content increases in the majority of cases. In SCGPC without SF, when the RCA content is between 0% and 100%, the peak strength is negatively affected by 4.34%, 8.72%, 11.5%, and 16.67%, while the peak deflection is negatively affected by 0.798%, -2.33%, -4.86%, and -8.91%. The percentages for peak strength and peak deflection for SCGPC with 1.5% SF content are -5.19%, -7.32%, -17.06%, and 12.86%, respectively. R100S1.5 has a more uniform structure with only one type of RCA inclusion, which contributes to its higher peak strength

compared to R75S1.5. The percentages for peak strength and peak deflection for SCGPC. An increase in the proportion of SF from 0% to 1.5% results in corresponding increases of 8.72%, 10.61%, and 15.81% in peak strength. On the contrary, there is a more substantial alteration in the peak deflection, denoting the extent to which the material can be bent before failure; it rises by 24.23%, 12.65%, and 18.42%, respectively.

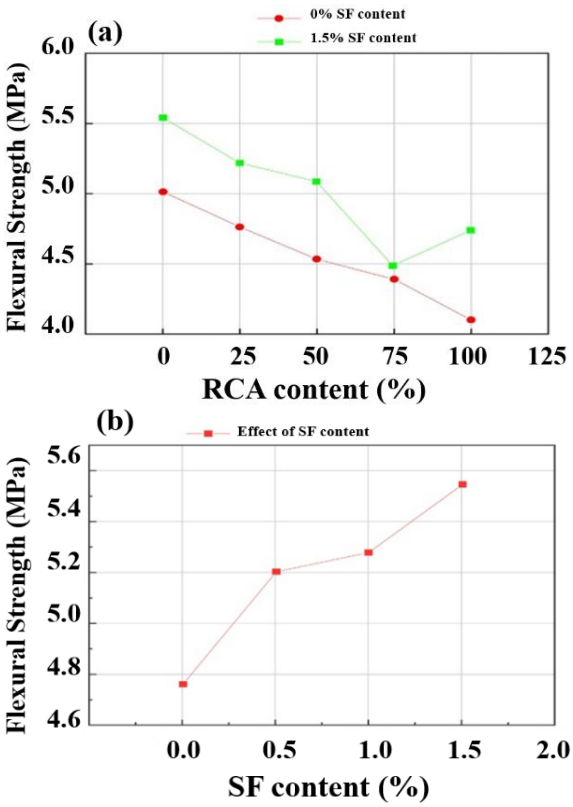

Figure 7. Flexural strength of SCGPC 's (a) Impact of RCA content; (b) Impact of SF ratio

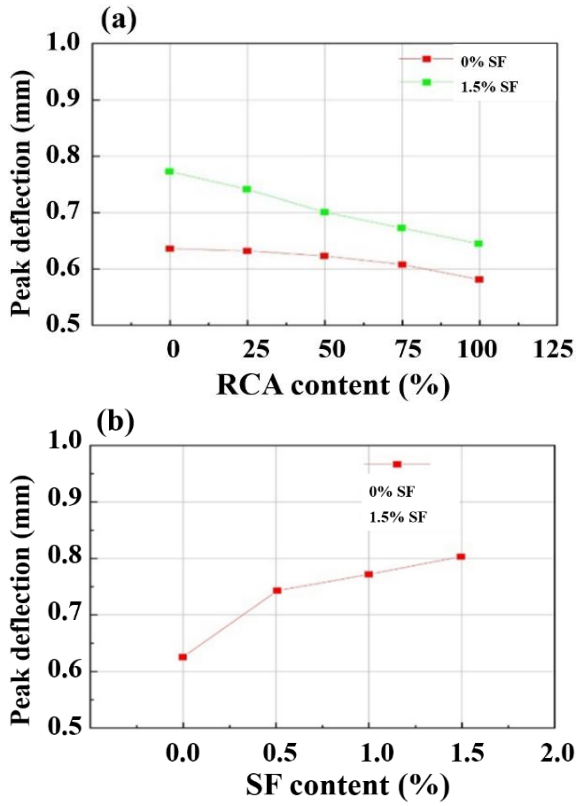

Figure 8. Flexural deflection of SCGPC's (a) Impact of RCA content; (b) Impact of SF content

Flexural toughness

Toughness is a valuable measure for assessing the ability of materials and structures to absorb energy when exposed to external forces. Figure 9 demonstrates the impact of the contents of RCA and SF on the flexural toughness of RCA. The fluctuation tendency of SCGPC's toughness is in accordance with that of its flexural strength and deflection. The influence of RCA and SF contents on $\Omega_{L/300}$ is determined to be minimal due to the presence of identical ascending branches of SCGPC. For a given RCA, SCGPC mixes including 1.5% steel fiber generated a first crack load that was roughly 4% and 5% higher, respectively, than similar companion blends containing 0.5% steel fiber. The influence of several descending branches of SCGPC becomes evident for $\Omega_{L/150}$ and $\Omega_{L/100}$. Furthermore, when the RCA percentage is less than 50%, the disparities between them are minimal due to the restricted harm caused by RCA at low concentrations. Comparable findings are also evident for SCGPC containing 0.5% and 1.5% SF. The observation illustrates that the inclusion of SF in RCA only improves the structural integrity of the concrete. While the fibers do help bridge cracks, they also introduce initial flaws in the RCA, such as aggregating of fibers, fragile fiber-matrix ITZs, and holes that ultimately harm the SCGPC's matrix.

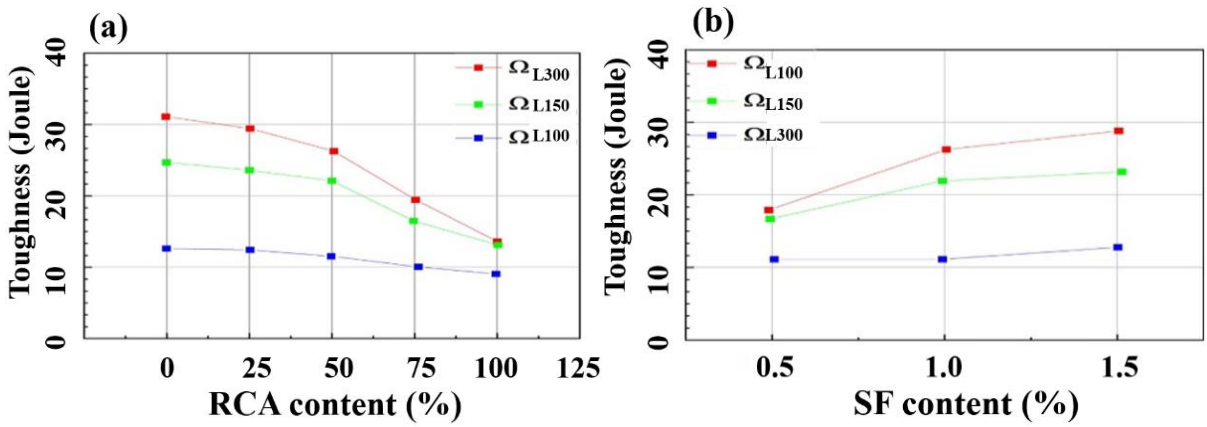

Figure 9. Flexural toughness of RCA. (a) Impact of RCA content; (b) Impact of SF content

4. DURABILITY INVESTIGATION OF SCGPC

4.1 Visual inspection

Specimens exposed to sulfuric acid solution

In order to assess the acid resistance of geopolymer concrete samples containing recycled coarse aggregate and steel fiber at varying concentrations (illustrated in Figure 10, they were subjected to a simulated acidic environment containing 5% H_2SO_4 for 56 days. Erosion was comprehensively assessed by careful visual examination and in-depth analysis. Upon visual examination, it was seen that all samples exposed to acid displayed substantial erosion. The group containing 50% recycled aggregate exhibited the most severe erosion, likely attributed to its increased porosity. The higher susceptibility is ascribed to the interconnected void network present in the aggregate, which facilitates the penetration of acid through more accessible channels. Meanwhile, the incorporation of steel fibers greatly lowered degradation in all samples. The presence of these fibers served as an internal reinforcement, impeding the creation of cracks and restricting the penetration of acid into the geopolymer matrix at greater depths.

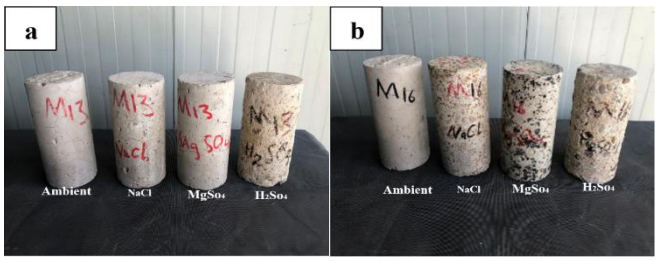

Figure 10. The visual characteristics of test specimens subjected to chemical attack for 56 days: (a) SCGPC with 50% RCA 0% SF; (b) SCGPC with 50% RCA 1.5% SF

Specimens exposed to magnesium sulfate ($MgSo_4$) and seawater (NaCl) solutions

Geopolymer concrete samples were immersed in solutions of magnesium sulphate ($MgSO_4$) and seawater (NaCl) for 56 days. Visual observations were made to assess visible changes, and their structural integrity was examined. Figure 10(a) depicts the samples without steel fiber reinforcing. These samples showed no apparent change after being immersed in magnesium sulphate and seawater, indicating that their structural integrity was preserved throughout the immersion. Figure 10(b) shows the samples that were strengthened with steel fibers. The surface of the concrete turned brown in seawater and black in magnesium sulphate solution. These colour variations can be traced to the solution's interaction with the steel fibers, which discolors the concrete surface.

Weight loss

The work studied how the weight of SCGPC changes over time. The weight of the concrete at different ages was compared to its initial weight. Weight changes relative to the initial weight is called WLF. To measure WLF accurately, firstly, deposits from the surface of the concrete was removed. Interestingly, it is found that SCGPC lasts longer (is more durable) when the WLF is lower. In other words, less weight loss over time indicates higher durability of SCGPC [45]. Weight variations in geopolymer concrete samples during 56 days were recorded. The control samples were used to compare with samples subjected to different solutions. Figure 11(a) depicts the weight variations of control samples over time, which reveal a reduction due to continual hydration responses. The study focused on comparing weight changes between different samples, highlighting the large weight loss in the RCA50SF0 sample and the low weight change in the 0RCA1.5SF. The weight fluctuations of samples exposed to 5% concentrated sulfuric acid for a duration of 56 days are illustrated in Figure 11(b).

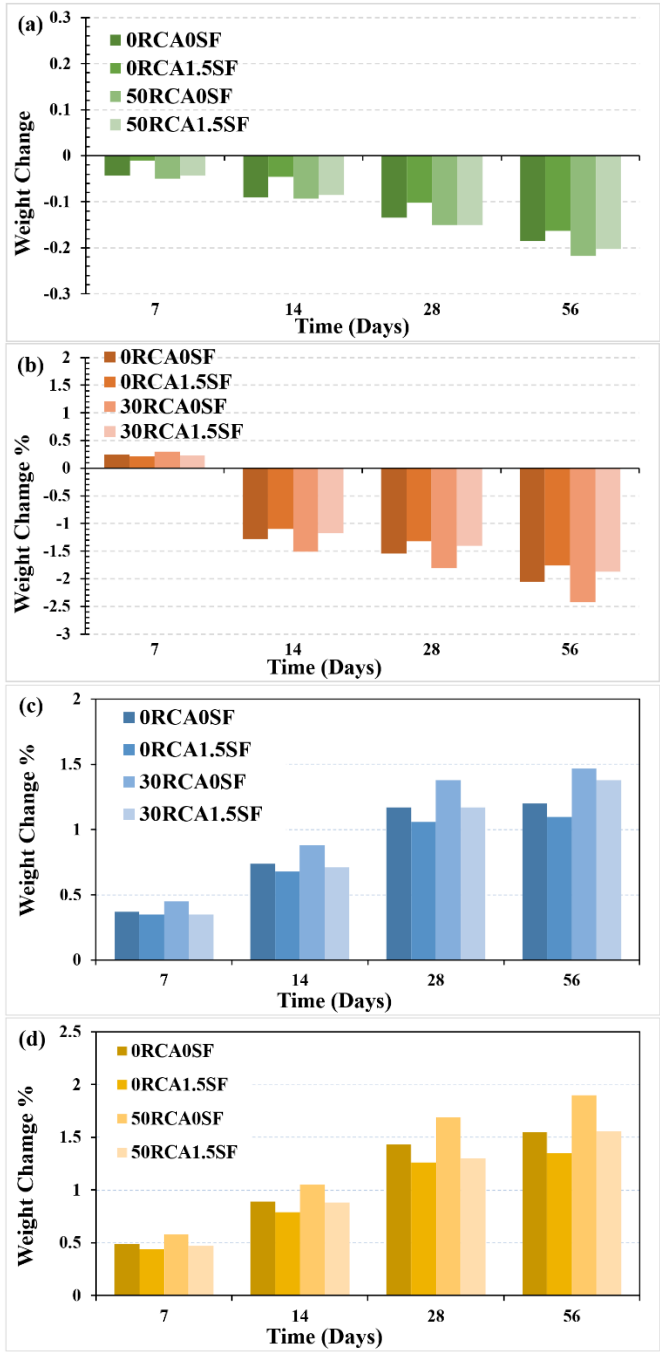

Figure 11. Weight change of the specimens under different environment: (a) Specimens at ambient environment; (b) Specimens exposed to sulfuric acid; (c) Specimens exposed to seawater; (d) Specimens exposed to $MgSO_4$

On the contrary, the weight of acid-immersed samples increased gradually over the course of the initial week, with the maximal gains of 0.25%, 0.22%, 0.3%, and 0.23% observed for samples labelled RCA0SF0, RCA0SF1.5, RCA50SF0, and RCA50SF1.5, respectively. However, after the initial week, the samples experienced a significant decline

in weight as a result of alkalis and other components of the concrete dissolving in the acidic environment. Weight losses of 2.05%, 1.76%, 2.42%, and 1.87% were documented for the RCA0SF0, RCA0SF1.5, RCA50SF0, and RCA50SF1.5 samples, respectively, after a period of 56 days. It is worth mentioning that the RCA50SF0 sample underwent more pronounced attrition as a consequence of the elevated RCA content, which led to improved porosity and permeability. SCGPC samples with different concentrations of RCA and SF were produced and submerged for 56 days in a solution containing 5% magnesium sulphate and 3.5% seawater. Weight fluctuations of the specimens were monitored and documented at regular intervals during the immersion phase. The weight variations of the geopolymer concrete samples that were submerged in the seawater and magnesium sulphate solution for 56 days, respectively, are illustrated in Figures 11 (c) and (d). Weight gains were observed in all samples, and the corresponding values were documented. 1.10% (RCA0SF1.5), 1.47% (RCA50SF0), and 1.38% (RCA50SF1.5) for seawater. 1.45% (RCA0SF0), 1.35% (RCA0SF1.5), 1.90% (RCA50SF0), and 1.56% (RCA50SF1.5) for magnesium sulphate solution. Weight increases were greatest in samples with a greater concentration of RCA, such as RCA50SF0, as a result of increased porosity.

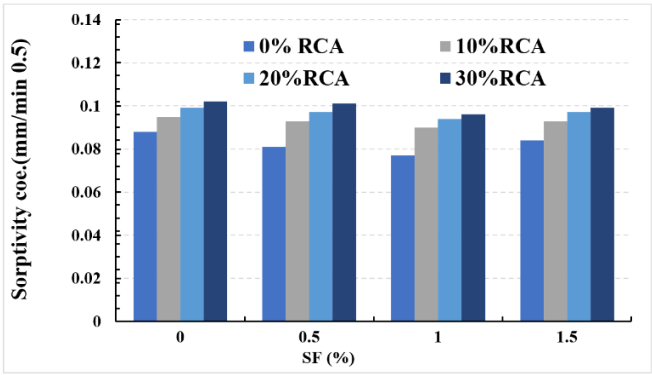

Figure 12. Rate of water absorption on different SCGPCs samples

Determining concrete's longevity requires knowledge of its moisture absorption and transport properties. To further understand this process, the sorptivity test is highly recommended. It is useful for assessing the capillary characteristics of concrete since it quantifies the rate of water absorption by the material. Figure 12 displays sorptivity values for different samples of SCGPCs at 28 days. Higher sorptivity values indicate a material's greater tendency to absorb water by capillary action. Figure 12 shows that increasing RCA in the samples results in higher sorptivity values. In contrast, the introduction of 1% SF appears to somewhat reduce sorptivity compared to samples without fibers, as seen in sample 'RCA0SF1', which has the lowest sorptivity value (5.6) of those examined. Thus, there is a positive correlation between RCA concentration and water absorption. Water absorption rises by 5%, 6%, and 15% as the RCA ratios increase (0.10, 0.20, and 0.30). This supports the idea that RCA's porous nature improves capillary action in concrete, resulting in increased water uptake. The study investigated the impact of steel fiber content on water absorption at concentrations of 0%, 0.5%, 1%, and 1.5%. The inclusion of steel fibers in samples seems to exert a moderate inhibitory impact on sorptivity, as illustrated in Figure 12, in comparison to samples lacking fibers. The reason for this is the function of the fibers, which is to obstruct water pathways within the concrete matrix, thereby decreasing the rate at which water enters [38]. It is noteworthy that Figure 12 proposes that a ratio of 1% steel fiber might be most effective in reducing water absorption.

Strength loss

In general, the compressive strength of specimens diminishes as the curing age increases in an acidic, sulfate and chloride environment [29, 46]. Figure 13 depicts the results of the compressive strength tests conducted on the SCGPCs specimens in various conditions, including the control environment, 3.5% saltwater, 5% magnesium sulfate, and 5% sulfuric acid. Following the corresponding chemical exposure, the residual compressive strengths (percent) of the specimens were denoted by numbers at the top of each relevant graphic data set. For each concrete specimen, the average compressive strength was determined using identical samples. The results show that samples with 0% RCA and 1.5% SF have the highest compressive strength, whereas samples with 50% RCA and 0% SF have the lowest strength. Furthermore, the compressive strength of samples with (RCA0SF0), (RCA0SF1.5), (RCA50SF0), and (RCA50SF1.5) dropped by 3%, 4%, 3%, and 0%, respectively, when exposed to 3.5% sodium chloride (NaCl). In a similar vein, the aforementioned samples experienced strength reductions of 11%, 6%, 12%, and 1% when exposed to 5% magnesium sulfate ($MgSO_4$). Lastly, 5% sulfuric acid (H_2SO_4) treatment resulted in respective strength reductions of 20%, 17%, 25%, and 12%. It was discovered that the elevated RCA ratio contributed to a greater gap percentage and absorption, which ultimately resulted in a more severe degradation of the sample [15].

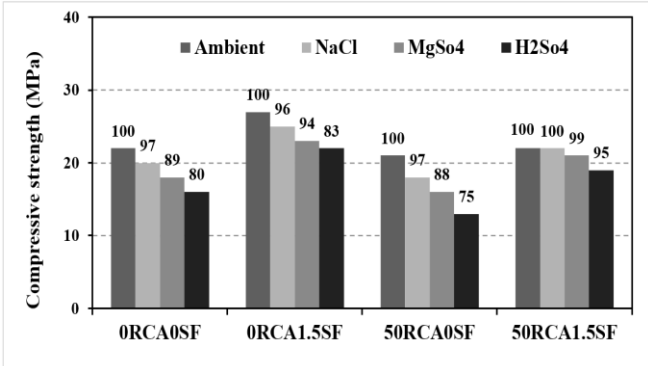

Figure 13. Residual strength of SCGPC composites after exposure to NaCl, $MgSO_4$, and H_2SO_4 solution

Microstructural investigations

The comparison of the microstructures of geopolymer specimens prior to and subsequent to the chemical attack involving acid, sulphate, and seawater studied with SEM. As seen in Figure 14(a), the image illustrates the compact structure of the control sample embedded in the geopolymer matrix, which suggests geopolymerization and the potential for geopolymer composites to be strengthened due to the strong bonds between the geopolymer materials. The microscopy alterations of geopolymer specimens subsequent to a 56-day exposure to solutions containing 5% H_2SO_4, 3% NaCl, and $MgSO_4$, respectively, are depicted in Figures 14(b-d). As illustrated in Figure 14(b), the geopolymer samples that were immersed in H_2SO_4 solution demonstrated a significantly greater level of degradation in comparison to the other samples. This degradation was attributed to the formation of gypsum

crystals [47]. Furthermore, it has been reported by Maes and De Belie [48] that microstructural degradation was associated with an increased quantity of recently generated microcracks, some of which were enlarged and partially filled with gypsum crystals. As illustrated in Figure 14 (c), the circumstance changed significantly after $MgSO_4$ exposure. A marginal development of ettringite was detected in the geopolymer mixtures, as evidenced by this micrograph. The reaction between external SO_4^{2-} and the dissolved calcium and aluminium from the reacted alkali activator produces ettringite [49]. Conversely, geopolymer samples immersed in NaCl did not exhibit any notable development of new distinct phases or specific alterations in morphology. The results obtained from exposure to H_2SO_4 and $MgSO_4$ were the subject of internal disintegrating stresses induced by gypsum crystals within the geopolymer matrix. These stresses resulted in cracking, spalling, and accelerated deterioration, as documented in reference [25].

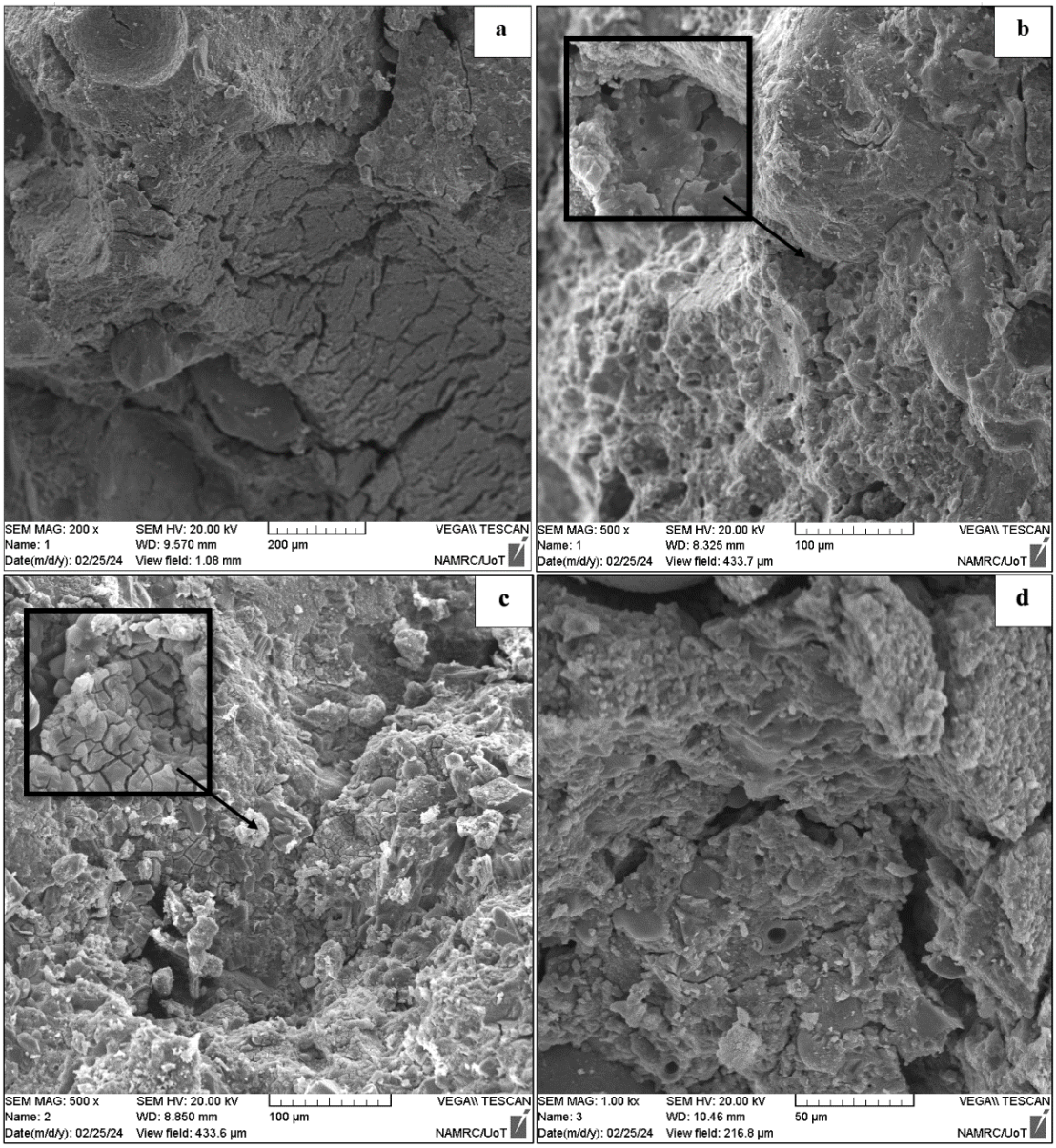

Figure 14. SEM images of specimens (a) In ambient condition, after 56-days exposure to (b) H_2SO_4; (c) $MgSO_4$; and (d) 3.5% Seawater

Challenges and considerations:

- **Synergy of RCA and Steel Fibers:** The negative synergy between RCA and steel fibers for compressive and tensile strength is a substantial barrier. More research is needed to understand the mechanisms underlying this interaction and devise measures to mitigate it. This could include experimenting with different fiber types, surface treatments, or optimizing the mix design to improve the bond between the RCA, fibers, and geopolymer matrix.
- **Durability Concerns with RCA:** The study suggests that RCA may reduce the SCGPC's overall durability, particularly under stress. More extensive durability testing, including freeze-thaw cycles and long-term chemical exposure, is critical. Furthermore, researching ways to increase the interfacial interaction between RCA and the geopolymer matrix may improve long-term performance**.**
- **Reduced dependency on natural materials:** The effective application of RCA in SCGPC provides a viable method for lowering reliance on natural aggregates, which have a major environmental impact due to extraction and processing.
- **Geopolymers as a Sustainable Alternative:** This study demonstrates geopolymers' promise as a more sustainable alternative to typical Portland cement concrete.

Geopolymer manufacture often produces fewer CO_2 emissions and can use industrial byproducts as basic materials.

By addressing the issues raised in this study, the viability of utilizing RCA in steel fiber-reinforced SCGPC can be increased. This will help to considerably advance the development of more sustainable construction materials with appropriate mechanical qualities and durability.

Future research directions:

Based on existing current research on below are some prospective future study ideas:

Optimizing mix design:

- Investigate the impact of various recycled aggregates (e.g., crushed concrete, brick) on the characteristics of SCGPC.
- Investigate the utilization of different steel fiber shapes (e.g., hooked, crimped) and their effects on mechanical performance and workability.
- Investigate the effects of various metakaolin supplies and activation methods on the overall performance of SCGPC.

Durability under extreme conditions:

- Examine the long-term behavior of SCGPC under freeze-thaw cycles, salt exposure, and harsh chemical conditions.
- Examine the fire resistance of SCGPC with recycled aggregates and steel fibers versus standard concrete.
- Assess SCGPC's carbonation resistance and its impact on long-term durability.

Sustainability aspects:

- Perform a life cycle assessment (LCA) to compare the environmental impact of SCGPC using recycled aggregates and steel fibers to traditional concrete.
- Consider employing industrial leftovers or waste materials as partial substitutes for metakaolin in the binder.
- Create cost-effective methods for pre-treating recycled aggregates to assure compatibility with the geopolymer matrix.

Advanced characterization techniques:

- Use microstructural analytical techniques such as X-ray diffraction (XRD) and scanning electron microscopy (SEM) to better understand the interaction of recycled aggregates, steel fibers, and the geopolymer matrix.
- Use computer modeling to anticipate the mechanical behavior of SCGPC under various loading circumstances.
- Create non-destructive testing methods to assess the health and performance of SCGPC structures in situ.

5. CONCLUSION

1) All mixes met EFNARC standards for flow, T_{50}, and filling ratio. Mixes that passed the flow requirement met the other two requirements as well.

2) With an increase in RCA content, SCGPC often exhibits a drop in compressive and splitting tensile strengths and flexural characteristics, whereas an increase in SF content results in an improvement. Compressive strength is less affected by SF content than splitting tensile and flexural values.

3) Both the compressive and splitting tensile strengths of RCA are negatively affected by the synergistic effect. Although there is a clear positive correlation between the flexural performance metrics. When it comes to SCGPC's flexural properties, the favorable effect of SF more than makes up for the negative effect of RCA.

4) Regarding durability, the findings demonstrate that immersing SCGPC in chemicals for 56 days had varying effects on their weight and compressive strength, according to the kind of geopolymer and chemical solution used.

- Weight gains were observed in all samples, and the corresponding values were documented. 1.10% (0RCA1.5SF), 1.47% (50RCA0SF), and 1.38% (50RCA1.5SF) for seawater. 1.45% (0RCA0SF), 1.35% (0RCA1.5SF), 1.90% (50RCA0SF), and 1.56% (50RCA1.5SF) for magnesium sulphate solution. Weight increases were greatest in samples with a greater concentration of RCA, such as 50RCA0SF, as a result of increased porosity.
- When comparing various forms of geopolymer, it becomes clear that including fibers can improve the durability of the material. The decreased rate of strength degradation seen in fiber-reinforced geopolymer (SCFRG) compared to plain geopolymer (SCGPC) demonstrates this advantage.
- Regarding the visual examination, the geopolymer shows minimal changes when exposed to seawater and $MgSO_4$. The interaction between geopolymer and H_2SO_4 results in discolouration, a porous surface, expansion, and fracturing. These effects are caused by the dissolving of reactive elements and the creation of sulfur dioxide and gypsum crystals.
- This research aimed to investigate the combined effect of recycled coarse aggregate (RCA) and steel fibers (SF) in a metakaolin-based geopolymer concrete (SCGPC). Existing research primarily focused on natural coarse aggregates, and this study aimed to fill the knowledge gap regarding RCA's interaction with steel fibers within a geopolymer matrix.
- The findings directly address the research objectives.
- **Workability**: All mixes achieved the required workability standards, indicating successful self-compacting behavior (Objective: Investigate the impact of combined utilization).
- **Mechanical Performance**: The study confirmed the expected trends: increasing RCA content generally decreased compressive and flexural strength, while steel fibers improved these properties. However, the impact of steel fibers was less pronounced on compressive strength compared to splitting tensile and flexural strengths (Objective: Investigate how this combination affects the mechanical qualities).
- **Synergy between RCA and SF**: An interesting finding was the negative synergy between RCA and SF for compressive and splitting tensile strengths. Conversely, a positive synergy was observed for flexural performance, where the benefit of steel fibers outweighed the negative effect of RCA (Objective: Investigate how RCA interacts with steel fibres in a metakaolin geopolymer matrix).
- **Durability**: The research examined the effect of harsh environments (acidic and salty) on SCGPC. While weight gain was observed in all samples, the extent of change varied depending on the geopolymer mix and the specific chemical solution. Importantly, the inclusion of steel fibers improved the overall durability as evidenced by a reduced rate of strength degradation in fiber-reinforced geopolymer compared to plain geopolymer. Visual examination revealed minimal changes for seawater and magnesium sulfate exposure, while sulfuric acid exposure caused significant surface degradation and cracking (Objective: Investigate ... durability).

In conclusion, the research successfully addressed the knowledge gap regarding the combined effects of RCA and steel fibers in a metakaolin-based geopolymer concrete. The findings provide valuable insights for developing sustainable construction materials using recycled components while

maintaining good mechanical performance and durability.

REFERENCES

[1] Singh, N.B., Middendorf, B. (2020). Geopolymers as an alternative to Portland cement: An overview. Construction and Building Materials, 237: 117455. https://doi.org/10.1016/j.conbuildmat.2019.117455

[2] Ranjbar, N., Zhang, M. (2020). Fiber-reinforced geopolymer composites: A review. Cement and Concrete Composites, 107: 103498. https://doi.org/10.1016/j.cemconcomp.2019.103498

[3] Zhang, B. (2024). Durability of sustainable geopolymer concrete: A critical review. Sustainable Materials and Technologies, e00882. https://doi.org/10.1016/j.susmat.2024.e00882

[4] Zhao, C., Li, Z., Peng, S., Liu, J., Wu, Q., Xu, X. (2024). State-of-the-Art review of geopolymer concrete carbonation: From impact analysis to model establishment. Case Studies in Construction Materials, e03124. https://doi.org/10.1016/j.cscm.2024.e03124

[5] Singh, R.P., Vanapalli, K.R., Cheela, V.R.S., Peddireddy, S.R., Sharma, H.B., Mohanty, B. (2023). Fly ash, GGBS, and silica fume based geopolymer concrete with recycled aggregates: Properties and environmental impacts. Construction and Building Materials, 378: 131168. https://doi.org/10.1016/j.conbuildmat.2023.131168

[6] Pradhan, P., Panda, S., Parhi, S.K., Panigrahi, S.K. (2022). Factors affecting production and properties of self-compacting geopolymer concrete-A review. Construction and Building Materials, 344: 128174. https://doi.org/10.1016/j.conbuildmat.2022.128174

[7] Thakur, M., Bawa, S. (2022). Self-compacting geopolymer concrete: A review. Materials Today: Proceedings, 59: 1683-1693. https://doi.org/10.1016/j.matpr.2022.03.400

[8] Jeyaseela, J. (2024). Study on workability and durability characteristics of self-compacting geopolymer concrete composites. Research Square. https://doi.org/10.21203/rs.3.rs-3942681/v1

[9] Vishnu, N., Kolli, R., Ravella, D.P. (2021). Studies on self-compacting geopolymer concrete containing flyash, GGBS, wollastonite and graphene oxide. Materials Today: Proceedings, 43: 2422-2427. https://doi.org/10.1016/j.matpr.2021.02.142

[10] Wang, F., Kovler, K., Provis, J.L., Buchwald, A., Cyr, M., Patapy, C., Kamali-Bernard, S., Courard, L., Sideris, K. (2018). Metakaolin. Properties of Fresh and Hardened Concrete Containing Supplementary Cementitious Materials: State-of-the-Art Report of the RILEM Technical Committee 238-SCM, Working Group. Springer, Cham, 4: 153-179. https://doi.org/10.1007/978-3-319-70606-1_5

[11] Sabir, B.B., Wild, S., Bai, J. (2001). Metakaolin and calcined clays as pozzolans for concrete: A review. Cement and Concrete Composites, 23(6): 441-454. https://doi.org/10.1016/S0958-9465(00)00092-5

[12] Ahmad, J., Majdi, A., Babeker Elhag, A., Deifalla, A.F., Soomro, M., Isleem, H.F., Qaidi, S. (2022). A step towards sustainable concrete with substitution of plastic waste in concrete: Overview on mechanical, durability and microstructure analysis. Crystals, 12(7): 944. https://doi.org/10.3390/cryst12070944

[13] El Jery, A., Salman, H.M., Al-Khafaji, R.M., Nassar, M.F., Sillanpää, M. (2023). Thermodynamics Investigation and artificial neural network prediction of energy, exergy, and hydrogen production from a solar thermochemical plant using a polymer membrane electrolyzer. Molecules, 28(6): 2649. https://doi.org/10.3390/molecules28062649

[14] Siddique, R., Klaus, J. (2009). Influence of metakaolin on the properties of mortar and concrete: A review. Applied Clay Science, 43(3-4): 392-400. https://doi.org/10.1016/j.clay.2008.11.007

[15] Ahmad, J., González-Lezcano, R.A., Majdi, A., Ben Kahla, N., Deifalla, A.F., El-Shorbagy, M.A. (2022). Glass fibers reinforced concrete: Overview on mechanical, durability and microstructure analysis. Materials, 15(15): 5111. https://doi.org/10.3390/ma15155111

[16] Mozafarjazi, M., Rabiee, R. (2024). Experimental and numerical study on the load-bearing capacity, ductility and energy absorption of RC shear walls with opening containing zeolite and silica fume. Engineering Solid Mechanics, 12(3): 237-246. http://dx.doi.org/10.5267/j.esm.2024.1.009

[17] Farhan, K.Z., Johari, M.A.M., Demirboğa, R. (2020). Assessment of important parameters involved in the synthesis of geopolymer composites: A review. Construction and Building Materials, 264: 120276. https://doi.org/10.1016/j.conbuildmat.2020.120276

[18] Li, B., Yu, S., Gao, B., Li, Y., Wu, F., Xia, D., Chi, Y., Wang, S. (2023). Effect of recycled aggregate and steel fiber contents on the mechanical properties and sustainability aspects of alkali-activated slag-based concrete. Journal of Building Engineering, 66: 105939. https://doi.org/10.1016/j.jobe.2023.105939

[19] Le, H.B., Bui, Q.B., Tang, L. (2021). Geopolymer recycled aggregate concrete: From experiments to empirical models. Materials, 14(5): 1180. https://doi.org/10.3390/ma14051180

[20] Hemmati, M., Messadi, T., Gu, H., Seddelmeyer, J., Hemmati, M. (2024). Comparison of embodied carbon footprint of a mass timber building structure with a steel equivalent. Buildings, 14(5): 1276. https://doi.org/10.3390/buildings14051276

[21] Zhang, G., Ali, Z.H., Aldlemy, M.S., Mussa, M.H., Salih, S.Q., Hameed, M.M., Al-Khafaji, Z.S., Yaseen, Z.M. (2022). Reinforced concrete deep beam shear strength capacity modelling using an integrative bio-inspired algorithm with an artificial intelligence model. Engineering with Computers, 38(Suppl1): 15-28. https://doi.org/10.1007/s00366-020-01137-1

[22] Xu, Z., Huang, Z., Liu, C., Deng, X., Hui, D., Deng, S. (2021). Research progress on mechanical properties of geopolymer recycled aggregate concrete. Reviews on Advanced Materials Science, 60(1): 158-172. https://doi.org/10.1515/rams-2021-0021

[23] Al-Farhany, K., Abdulkadhim, A., Hamzah, H.K., Ali, F.H., Chamkha, A. (2022). MHD effects on natural convection in a U-shaped enclosure filled with nanofluid-saturated porous media with two baffles. Progress in Nuclear Energy, 145: 104136. https://doi.org/10.1016/j.pnucene.2022.104136

[24] Mesgari, S., Akbarnezhad, A., Xiao, J.Z. (2020). Recycled geopolymer aggregates as coarse aggregates for Portland cement concrete and geopolymer concrete:

Effects on mechanical properties. Construction and Building Materials, 236: 117571. https://doi.org/10.1016/j.conbuildmat.2019.117571
[25] Ren, D., Yan, C., Duan, P., Zhang, Z., Li, L., Yan, Z. (2017). Durability performances of wollastonite, tremolite and basalt fiber-reinforced metakaolin geopolymer composites under sulfate and chloride attack. Construction and Building Materials, 134: 56-66. https://doi.org/10.1016/j.conbuildmat.2016.12.103
[26] Younis, K.H. (2021). Metakaolin modified recycled aggregate concrete containing recycled steel fibers. Materials Today: Proceedings, 45: 4689-4694. https://doi.org/10.1016/j.matpr.2021.01.120
[27] Alvarez, G.L., Nazari, A., Bagheri, A., Sanjayan, J.G., De Lange, C. (2017). Microstructure, electrical and mechanical properties of steel fibres reinforced cement mortars with partial metakaolin and limestone addition. Construction and Building Materials, 135: 8-20. https://doi.org/10.1016/j.conbuildmat.2016.12.170
[28] Samawi, K.A., Salman, E.A.A., Alshekhly, B.A.A., Nassar, M.F., Borzehandani, M.Y., Abdulkareem-Alsultan, G., Alif Mohammad Latif, M., Abdulmalek, E. (2022). Rational design of different π-bridges and their theoretical impact on indolo [3, 2, 1-jk] carbazole based dye-sensitized solar cells. Computational and Theoretical Chemistry, 1212: 113725. https://doi.org/10.1016/j.comptc.2022.113725
[29] Kanagaraj, B., Anand, N., Alengaram, U.J., Raj, R.S. (2023). Engineering properties, sustainability performance and life cycle assessment of high strength self-compacting geopolymer concrete composites. Construction and Building Materials, 388: 131613. https://doi.org/10.1016/j.conbuildmat.2023.131613
[30] Parsaee, F., Fayzullaev, N., Nassar, M.F., Abd Alreda, B., Mahmoud, H.M., Taki, A.G., Faraji, M. (2024). Co-Fe dual-atom isolated in N-doped graphydine as an efficient sulfur conversion catalyst in Li-S batteries. Journal of Alloys and Compounds, 988: 174136. https://doi.org/10.1016/j.jallcom.2024.174136
[31] Samawi, K.A., Abdulrazzaq, S.J., Zorah, M., Al-Bahrani, M., Mahmoud, H.M., Abdulkareem-Alsultan, G., Taki, A.G., Nassar, M.F. (2024). MoS2/graphdiyne nanotube/MXene 3D-interconnected ternary aerogel: A high-performance electrocatalyst for hydrogen evolution reaction. Journal of Solid State Chemistry, 334: 124690. https://doi.org/10.1016/j.jssc.2024.124690
[32] Samawi, K.A., Mohammed, B.A., Salman, E.A.A., Mahmoud, H.M., Sameen, A.Z., Mohealdeen, S.M., Abdulkareem-Alsultan, G., Nassar, M.F. (2024). Vertical growth of a 3D Ni-Co-LDH/N-doped graphene aerogel: a cost-effective and high-performance sulfur host for Li-S batteries. Physical Chemistry Chemical Physics, 26(12): 9284-9294. https://doi.org/10.1039/D3CP05716J
[33] Samawi, K.A., Salman, E.A.A., Hasan, H.A., Mahmoud, H.M., Mohealdeen, S.M., Abdulkareem-Alsultan, G., Abdulmalek, E., Nassar, M.F. (2024). Single-atom cobalt encapsulated in carbon nanotubes as an effective catalyst for enhancing sulfur conversion in lithium-sulfur batteries. Molecular Systems Design & Engineering, 9(5): 464-476. https://doi.org/10.1039/D3ME00191A
[34] Majdi, H.S., Shubbar, A.A., Nasr, M.S., Al-Khafaji, Z.S., Jafer, H., Abdulredha, M., Al Masoodi, Z., Sadique, M., Hashim, K. (2020). Experimental data on compressive strength and ultrasonic pulse velocity properties of sustainable mortar made with high content of GGBFS and CKD combinations. Data in Brief, 31. https://doi.org/10.1016/j.dib.2020.105961
[35] Xie, T., Gholampour, A., Ozbakkaloglu, T. (2018). Toward the development of sustainable concretes with recycled concrete aggregates: Comprehensive review of studies on mechanical properties. Journal of Materials in Civil Engineering, 30(9): 04018211. https://doi.org/10.1061/(ASCE)MT.1943-5533.0002304
[36] Shubbar, A.A., Sadique, M., Nasr, M.S., Al-Khafaji, Z.S., Hashim, K.S. (2020). The impact of grinding time on properties of cement mortar incorporated high volume waste paper sludge ash. Karbala International Journal of Modern Science, 6(4): 7. https://doi.org/10.33640/2405-609X.2149
[37] Iqbal, S., Ali, A., Holschemacher, K., Bier, T.A. (2015). Mechanical properties of steel fiber reinforced high strength lightweight self-compacting concrete (SHLSCC). Construction and Building Materials, 98: 325-333. https://doi.org/10.1016/j.conbuildmat.2015.08.112
[38] Their, J.M., Özakça, M. (2018). Developing geopolymer concrete by using cold-bonded fly ash aggregate, nano-silica, and steel fiber. Construction and Building Materials, 180: 12-22. https://doi.org/10.1016/j.conbuildmat.2018.05.274
[39] Kou, S.C., Poon, C.S., Etxeberria, M. (2014). Residue strength, water absorption and pore size distributions of recycled aggregate concrete after exposure to elevated temperatures. Cement and Concrete Composites, 53: 73-82. https://doi.org/10.1016/j.cemconcomp.2014.06.001
[40] Kaplan, G., Bayraktar, O.Y., Gholampour, A., Gencel, O., Koksal, F., Ozbakkaloglu, T. (2021). Mechanical and durability properties of steel fiber-reinforced concrete containing coarse recycled concrete aggregate. Structural Concrete, 22(5): 2791-2812. https://doi.org/10.1002/suco.202100028
[41] Sukontasukkul, P., Pomchiengpin, W., Songpiriyakij, S. (2010). Post-crack (or post-peak) flexural response and toughness of fiber reinforced concrete after exposure to high temperature. Construction and Building Materials, 24(10): 1967-1974. https://doi.org/10.1016/j.conbuildmat.2010.04.003
[42] Wu, Z., Shi, C., He, W., Wu, L. (2016). Effects of steel fiber content and shape on mechanical properties of ultra high performance concrete. Construction and Building Materials, 103: 8-14. https://doi.org/10.1016/j.conbuildmat.2015.11.028
[43] Al-Majidi, M.H., Lampropoulos, A.P., Cundy, A.B., Tsioulou, O.T., Alrekabi, S. (2019). Flexural performance of reinforced concrete beams strengthened with fibre reinforced geopolymer concrete under accelerated corrosion. In Structures. Elsevier, 19: 394-410. https://doi.org/10.1016/j.istruc.2019.02.005
[44] Li, B., Xu, L., Chi, Y., Huang, B., Li, C. (2017). Experimental investigation on the stress-strain behavior of steel fiber reinforced concrete subjected to uniaxial cyclic compression. Construction and Building Materials, 140: 109-118. https://doi.org/10.1016/j.conbuildmat.2017.02.094
[45] Sangeetha, A., Shanmugan, S., Alrubaie, A.J., Jaber, M. M., Panchal, H., Attia, M.E.H., Elsheikh, A.H., Mevada, D., Essa, F.A. (2023). A review on PCM and nanofluid

for various productivity enhancement methods for double slope solar still: Future challenge and current water issues. Desalination, 551: 116367. https://doi.org/10.1016/j.desal.2022.116367

[46] Mehta, A., Siddique, R. (2017). Sulfuric acid resistance of fly ash based geopolymer concrete. Construction and Building Materials, 146: 136-143. https://doi.org/10.1016/j.conbuildmat.2017.04.077

[47] Vafaei, M., Allahverdi, A., Dong, P., Bassim, N. (2018). Acid attack on geopolymer cement mortar based on waste-glass powder and calcium aluminate cement at mild concentration. Construction and Building Materials, 193: 363-372. https://doi.org/10.1016/j.conbuildmat.2018.10.203

[48] Maes, M., De Belie, N. (2014). Resistance of concrete and mortar against combined attack of chloride and sodium sulphate. Cement and Concrete Composites, 53: 59-72. https://doi.org/10.1016/j.cemconcomp.2014.06.013

[49] Ye, H., Chen, Z., Huang, L. (2019). Mechanism of sulfate attack on alkali-activated slag: The role of activator composition. Cement and Concrete Research, 125: 105868. https://doi.org/10.1016/j.cemconres.2019.105868